

On the Relation between the Interfacial Charge of a Discharging Nozzle and Electrification of a Liquid Microjet

Naoya Kurahashi and Toshinori Suzuki*

Department of Chemistry, Graduate School of Science, Kyoto University,
Kitashirakawa Oiwake-cho, Sakyo-ku, Kyoto 604-8502, Japan

E-mail: suzuki@kuchem.kyoto-u.ac.jp

A liquid microjet discharged from a fused silica capillary is electrified, and the polarity of this electrification is opposite to that of the net charge at the solid–liquid interface of the capillary nozzle.

Keywords: Liquid microjet | Fused silica | Capillary nozzle

Liquid microjets, cylindrical streams of liquid with a diameter of tens of micrometers, are now widely employed in photoelectron spectroscopy of liquids¹ and gas-surface scattering experiments.² The small surface area of the microjet minimizes evaporation of solvent molecules and facilitates introduction of volatile liquids into high-vacuum chambers. However, a liquid microjet is electrically charged, because the liquid flow shears off an electric double layer at the inner wall of a capillary nozzle to create unequal number densities of cations and anions in the mobile part of the flow (flow electrification).^{3,4}

In a previous study,⁵ we showed that the electric potential of a liquid microjet of NaX solution (X = Cl, Br, and I) varies with the electrolyte concentration. A notable common feature of the variation was that the polarity of the potential reverses at around a concentration of 30 mM (Figure 1), suggesting that Na⁺ plays a key role in determining the polarity. In the present work, we discuss the relation between the electric charge at the inner wall of a capillary and the microjet.

The electric potential (ϕ_d) in the diffuse region of an electric double layer is described by the Poisson–Boltzmann equation as follows,

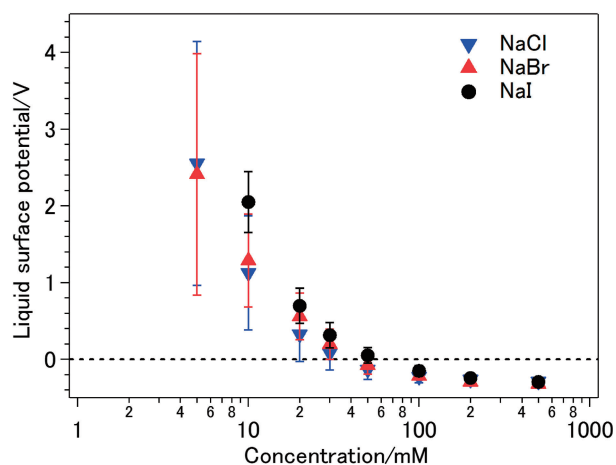


Figure 1. Surface potentials of liquid microjets of aqueous NaX solutions measured by photoelectron spectroscopy.⁵

$$\nabla^2 \phi_d = \frac{e}{\varepsilon_0 \varepsilon_r} \left(Z_+ N_+ e^{-\frac{eZ_+ \phi_d}{k_B T}} + Z_- N_- e^{-\frac{eZ_- \phi_d}{k_B T}} \right) \quad (1)$$

where e is the elementary charge, ε_0 and ε_r are respectively the permittivity of vacuum and the relative permittivity of a solution, Z_{\pm} and N_{\pm} are respectively the charge and number density of positive/negative ions, k_B is the Boltzmann constant, and T is the temperature. Equation 1 cannot be solved analytically. However, if the electric potential is sufficiently small such that the following condition holds, i.e.,

$$\left| \frac{eZ_{\pm} \phi_d(l)}{k_B T} \right| < 1 \quad (2)$$

an approximate solution can be expressed as

$$\phi_d(l) \approx \phi_{\text{OHP}} e^{-\kappa(l-l_{\text{OHP}})} \quad (3)$$

where l is the distance from the inner wall of the capillary, ϕ_{OHP} is the electric potential at the outer Helmholtz plane (OHP), and l_{OHP} is the position of the OHP. κ is the inverse of the Debye length, defined as

$$\kappa = \sqrt{\sum_i \frac{2Z_i^2 e^2 c}{\varepsilon_0 \varepsilon_r k_B T}} \quad (4)$$

where c is the concentration of the solution. ϕ_{OHP} is related to the interfacial charge ϕ_0 by

$$\phi_{\text{OHP}} = \phi_0 + \frac{\sigma_{\text{ad}}}{\varepsilon_0 \varepsilon_r} l_{\text{IHP}} - \frac{\sigma_{\text{surf}} + \sigma_{\text{ad}}}{2\varepsilon_0 \varepsilon_r} l_{\text{OHP}} \quad (5)$$

where σ_{surf} is the original charge density of the solid surface, σ_{ad} is the charge density of the adsorbed ions, and l_{IHP} is the position of the inner Helmholtz plane (IHP). The relative permittivity is assumed to be the same in all regions of the solution. Then, the continuity conditions for the electric field and the potential at the OHP yield

$$\phi_{\text{OHP}} = \frac{1}{\kappa} \frac{\sigma_{\text{surf}} + \sigma_{\text{ad}}}{2\varepsilon_0 \varepsilon_r} \quad (6)$$

If eq 2 holds, the charge density in the diffuse layer is given by

$$\rho \approx e \left(Z_+ |Z_-| c e^{\frac{eZ_+ \phi_d(l)}{k_B T}} + Z_- |Z_+| c e^{\frac{eZ_- \phi_d(l)}{k_B T}} \right) \quad (7)$$

Since $Z_+ = 1$ and $Z_- = -1$ for NaX, eq 7 simplifies to

$$\rho(l) \approx -2ce\phi_{\text{OHP}} e^{-\kappa(l-l_{\text{OHP}})} \quad (8)$$

This equation shows that the excess charge in a diffuse layer is opposite in sign to both ϕ_{OHP} and $\sigma_{\text{surf}} + \sigma_{\text{ad}}$. Although eq 3 is valid only for small ϕ_d , the opposite signs of ρ and $\sigma_{\text{surf}} + \sigma_{\text{ad}}$ are expected to be general.

In this study, we examine the relation between the signs of ρ and $\sigma_{\text{surf}} + \sigma_{\text{ad}}$ by measuring the streaming currents and surface

potentials of liquid microjets of aqueous NaI solutions using a chemically-modified fused silica capillary (GL Science FunCap-CE/Type A).^{6,7} This capillary has an amino group chemically bonded to a silanol (SiOH) group on a fused silica surface, so that $\sigma_{\text{surf}} + \sigma_{\text{ad}}$ is always positive at $\text{pH} \leq 7$ regardless of the concentration of NaI. After confirmation of the relation between ρ and $\sigma_{\text{surf}} + \sigma_{\text{ad}}$, we present a model that explains the reversal of a surface potential of a liquid microjet with the concentration of Na^+ .

A gradient-flow HPLC pump (JASCO PU-2089) was used to flow an aqueous NaI solution to a capillary nozzle. The capillary was inserted into a short section of PEEK tubing (inner diameter: 0.38 mm, outer diameter: 1/16 inch, length: 8.0 mm), leaving a 1.0-mm length of the capillary protruding from the tube, and was fixed using a 1/16 inch stainless-steel Swagelok fitting. This was then connected to the HPLC pump through a longer length of PEEK tubing (inner diameter: 0.13–0.25 mm, length: 1.5 m). After emerging from the capillary, the liquid microjet remained continuous for a length of about 3 mm, after which the jet disintegrated into droplets. The capillaries were passivated prior to experiments by flowing pure water (or aqueous NaI solution) for more than 2 hours. The sample solutions were prepared using ultrapure water (LC/MS grade, resistivity: 2 M Ω cm, Wako) and sodium iodide (99.5%, Wako). To measure the streaming current in air, a copper electrode was placed 5 mm or farther from the nozzle and the current flowing through it was monitored using a picoammeter (Keithley 6485/J). The actual electric potential of the microjet was measured in vacuum by He(I) photoelectron spectroscopy (PES) using a hemispherical electron energy analyzer (Scienta SES100). The design of our photoelectron spectrometer has been described in detail elsewhere,⁸ although the apparatus has been slightly modified such that the liquid microjet axis is vertical and the electron detection axis is horizontal. This modification has improved the vacuum conditions and enabled us to downsize the vacuum pump of the main chamber from a cryopump (20000 L s⁻¹) to a turbomolecular pump (2000 L s⁻¹). The liquid surface potential, Φ_{surf} , is calculated from the observed photoelectron kinetic energy (PKE) of water as follows,

$$\text{PKE} = h\nu - IE - \Phi_{\text{surf}} \quad (9)$$

where IE is the ionization energy.

Figure 2 shows streaming currents measured as functions of flow rate and NaI concentration for a capillary with a positive surface charge. As seen in the inset, pure water provides a negative streaming current (the microjet was negatively charged). Aqueous NaI solutions exhibit considerably smaller streaming currents, because of enhanced electroconductivity; however, the polarity of their current is always negative. We have also measured the liquid surface potential from the photoelectron energy shift of the 1b₁ band of gaseous water evaporated from the microjet of aqueous NaI solutions; the potentials of liquid microjets at concentrations of 15 and 100 mM were negative (−0.11 V). These results support the relation between ρ and $\sigma_{\text{surf}} + \sigma_{\text{ad}}$ described by eq 8.

As seen in Figure 1, the surface potential of a liquid microjet discharged from an unmodified fused silica capillary changes polarity at a concentration of about 30 mM NaX (X = Cl, Br, and I). Similar behavior has been reported by Lübcke and colleagues for a streaming current of NaX solutions.⁹ These

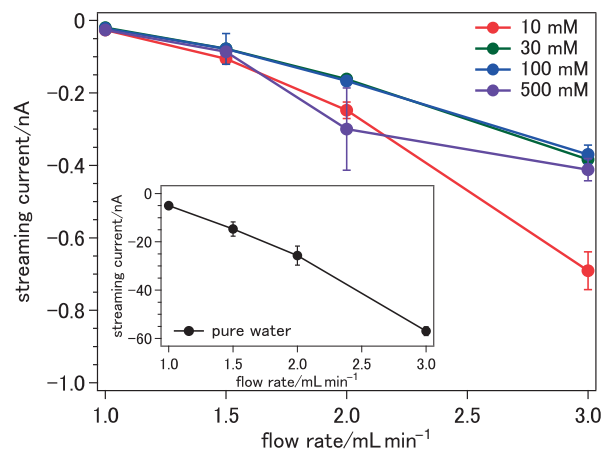


Figure 2. Flow rate dependence of streaming current discharged from the FunCap-CE/Type A capillary with a positive surface charge, measured at various NaI concentrations (0 to 500 mM). The negative sign of a streaming current corresponds to a negatively charged microjet. The nonlinearity of streaming currents is ascribed to a turbulent flow in the capillary.⁴

results are well explained, if we assume that the interfacial charge of fused silica changes polarity depending on the electrolyte concentration. The interface between fused silica and an aqueous solution is usually negatively charged. The most likely value of $\text{p}K_{\text{a}2}$ of silica is 4.5,¹⁰ and $\text{p}K_{\text{a}1}$ has been calculated as −0.25 from the isoelectric point ($\text{p}I = 2$)¹¹ and $K_{\text{a}2}$. Thus, in NaI 10 mM solution, the SiOH groups are expected to exist in the SiO^- , SiOH and SiOH_2^+ forms with a distribution of 74%, 26%, and 0%, respectively. Since SiOH_2^+ is not present at the silica surface in the neutral aqueous solution, it is considered that charge reversal is caused by sodium ions.

It is noted that fused silica is regarded as high-temperature-treated silica (HTT-silica), and that high temperature induces intermolecular dehydration of SiOH groups to generate siloxane (Si–O–Si) bonds.¹² The surface density of SiOH groups of HTT-silica has been estimated to be 0.7 nm⁻², while that of siloxane bonds is estimated to be as large as 12 nm⁻². Since the activation energy for hydrolysis of a siloxane bond is greater than 70 kJ mol⁻¹,¹³ its dissociation is negligible under our experimental conditions. Therefore, it is expected that the cations were preferentially adsorbed on SiO^- groups, while additional adsorption to siloxane bonds may have also been possible.

The adsorption equilibrium constant K can be predicted from the free energy change upon adsorption ΔG as follows,

$$\Delta G = -RT \ln K \quad (10)$$

In terms of the center–center distance between an adsorption site and an adsorbed cation r_{ad} , the change in the Coulomb potential energy upon adsorption onto this site is given by (Figure 3)

$$\Delta U = -\frac{e^2}{4\pi\epsilon_0\epsilon_r r_{\text{ad}}} \quad (11)$$

Several experimental and theoretical studies suggest that both a silica–solution interface and an adsorbed ion hold hydration shells.^{14,15} Thus, the distance between a SiOH site and an adsorbed cation is estimated to be 660 pm. The effective dielectric constant for water varies with electric field strength,

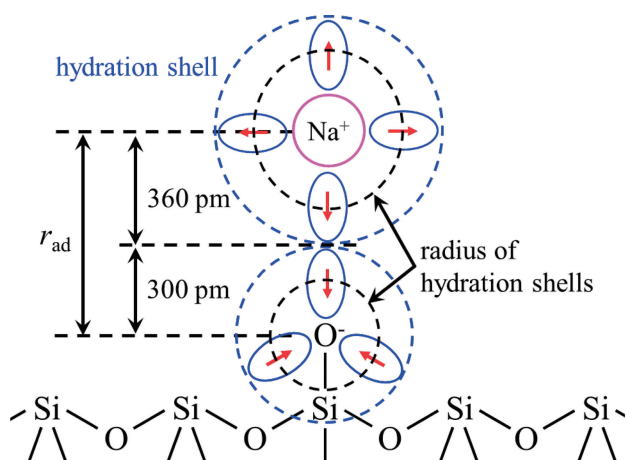
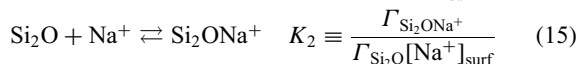
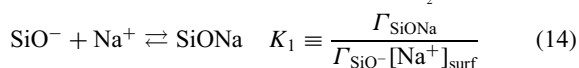
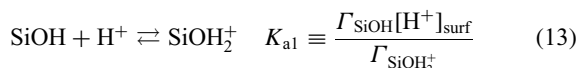
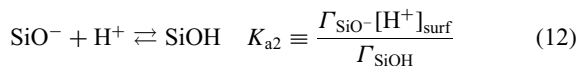


Figure 3. Schematic view of a sodium ion adsorbed on a negatively charged SiOH group. Blue ellipses show the hydration water molecules and red arrows show the direction of the permanent dipole moment of water. Black dashed lines indicate the radii of the hydration shells.

and the effective relative dielectric constant at the radius of the hydration shell is estimated to be 12 ± 3 .¹⁶ The change in the Coulomb potential energy is then calculated to be -17 ± 3 kJ mol⁻¹, in fair agreement with $\Delta G = -8.0$ kJ mol⁻¹ for sodium halide aqueous solutions and negatively charged SiOH groups.¹⁷

We consider the siloxane bond sites in a similar way. The properties of the surface siloxane bonds are expected to be similar to those of the disiloxane (SiH₃-O-SiH₃) molecule. The bond length for Si-O is 163.4 pm and the bond angle for Si-O-Si is 144.1°.¹⁸ From the dipole moment (0.24 D), the effective charge of silyl groups in disiloxane molecules is calculated to be $+0.050 e$, with the oxygen atom having a charge of $-0.10 e$. When the siloxane site and adsorbed ion are both hydrated, the effective relative permittivities are calculated to be approximately 75 around a siloxane bond and 40–45 around a cation.¹⁶ Using these values, the change in Coulomb potential energy was calculated to be -0.36 kJ mol⁻¹.

The chemical equilibria at the surface of HTT-silica are expressed as follows,



where Γ_X is the surface density of group X. From the ΔG values estimated earlier, we obtained K_1 and K_2 as 950 and 1.2, respectively. The total surface densities of silanol and siloxane are

$$\Gamma_{\text{Si}_2\text{O}} = \Gamma_{\text{SiO}^-} + \Gamma_{\text{SiOH}} + \Gamma_{\text{SiOH}_2^+} + \Gamma_{\text{SiONa}} \quad (16)$$

$$\Gamma_{\text{Si}_2\text{O}} = \Gamma_{\text{Si}_2\text{O}} + \Gamma_{\text{Si}_2\text{ONa}^+} \quad (17)$$

The surface ion densities $[X]_{\text{surf}}$ are determined from the Boltzmann equation using ϕ_{OHP} and the partition function N_X :

$$[\text{H}^+]_{\text{surf}} = N_{\text{H}^+} e^{-\frac{e\phi_{\text{OHP}}}{k_B T}} \quad (18)$$

$$[\text{Na}^+]_{\text{surf}} = N_{\text{Na}^+} e^{-\frac{e\phi_{\text{OHP}}}{k_B T}} \quad (19)$$

N_X is approximated as the bulk concentration c_X . Under the condition

$$\left| \frac{e\phi_{\text{OHP}}}{k_B T} \right| > 1 \quad (20)$$

$$\phi_{\text{OHP}} \approx \frac{\sigma_{\text{surf}} + \sigma_{\text{ad}}}{2\epsilon_0\epsilon_r} \frac{\ln\left(2e^{\frac{W(2)}{2}} - 1\right)}{K} \quad (21)$$

where $W(n)$ is the Lambert W function. The interfacial charge density is expressed as:

$$\sigma_{\text{surf}} + \sigma_{\text{ad}} = e(-\Gamma_{\text{SiO}^-} + \Gamma_{\text{Si}_2\text{ONa}^+}) \quad (22)$$

The coupled eqs 12–22 can be solved numerically to find ϕ_{OHP} , from which the surface density of each group and interfacial charge density can be calculated, as shown in Figures 4 and 5, respectively. The calculations reveal that the interfacial charge is zero at a concentration of 6.0 mM, negative at lower concentrations and positive at higher concentrations (Figures 4 and 5). Charge reversal has been observed due to the interaction of multivalent cations on a silica surface.^{19,20} However, sodium ions have not been considered to contribute to charge inversion.¹⁹ It is noted that previous experiments formed the flow path by chemical etching¹⁹ and acid washing,²⁰ which possibly resulted in a siloxane-free surface.

Our simulation shown in Figure 5 indicates that the interfacial charge density increases monotonically at concentration greater than 6 mM, while the liquid surface potential (Figure 1) is saturated at high concentration. This discrepancy may suggest that mutual interactions between the adsorbed Na⁺ ions, which we neglected in our model, hinder adsorption of Na⁺ at high concentrations.

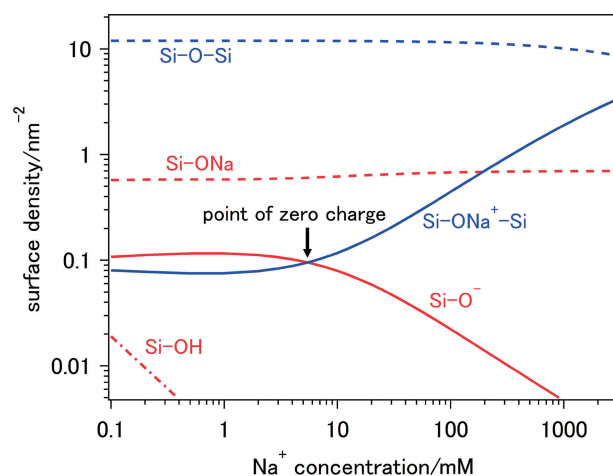


Figure 4. Calculated number density of surface groups of HTT-silica as a function of Na⁺ concentration. The apparent charge density is shown by the red and blue solid curves. The point at which the number density of red and blue are equal is the point of zero charge. The surface density of the positively charged silanol groups ($\Gamma_{\text{SiOH}_2^+}$) was almost zero at all concentrations.

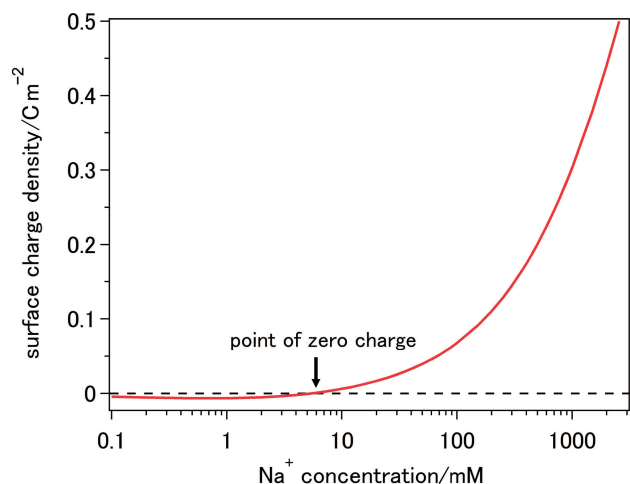


Figure 5. Calculated interfacial charge density of HTT-silica as a function of Na^+ concentration. The point of charge inversion is located at 6 mM Na^+ .

We have attempted to determine adsorption equilibrium constants from the temporal change in the potential when changing the salt concentration. However, we found that the first step is as fast or faster than the instrument's time resolution. In the near future, it will be necessary to measure the adsorption equilibrium constant by improving measurement time resolution. Since the electric potential of a microjet varies with the flow rate, and possibly with the actual dimensions of a capillary, we therefore demonstrate here only qualitative behavior for the charge reversal phenomenon based on the hypothesis of two adsorption sites on the fused silica surface. Further confirmation of this phenomenon requires determination of the equilibrium constants and spectroscopic detection of ion adsorption at the fused silica surface.

The authors thank Morihiko Onose, Junichi Nishitani, Christopher W. West, Shotaro Kudo, Ayano Hara, Ryuta Uenishi, and Stephan Thürmer for their experimental assistance.

Supporting Information is available on <http://dx.doi.org/10.1246/cl.170892>.

References

- 1 B. Winter, M. Faubel, *Chem. Rev.* **2006**, *106*, 1176.
- 2 D. K. Lancaster, A. M. Johnson, D. K. Burden, J. P. Wiens, G. M. Nathanson, *J. Phys. Chem. Lett.* **2013**, *4*, 3045.
- 3 S. Levine, J. R. Marriott, G. Neale, N. Epstein, *J. Colloid Interface Sci.* **1975**, *52*, 136.
- 4 W. L. Holstein, L. J. Hayes, E. M. C. Robinson, G. S. Laurence, M. A. Buntine, *J. Phys. Chem. B* **1999**, *103*, 3035.
- 5 N. Kurahashi, S. Karashima, Y. Tang, T. Horio, B. Abulimiti, Y. Suzuki, Y. Ogi, M. Oura, T. Suzuki, *J. Chem. Phys.* **2014**, *140*, 174506.
- 6 S. Kodama, A. Morikawa, K. Nakagomi, A. Yamamoto, A. Sato, K. Suzuki, T. Yamashita, T. Kemmei, A. Taga, *Electrophoresis* **2009**, *30*, 349.
- 7 Y. Iwamuro, R. Iio-Ishimaru, S. Chinaka, N. Takayama, S. Kodama, K. Hayakawa, *J. Health Sci.* **2010**, *56*, 606.
- 8 K. Nishizawa, K. Ohshimo, T. Suzuki, *J. Chin. Chem. Soc.* **2013**, *60*, 1403.
- 9 N. Preissler, F. Buchner, T. Schultz, A. Lübcke, *J. Phys. Chem. B* **2013**, *117*, 2422.
- 10 K. Leung, I. M. B. Nielsen, L. J. Criscenti, *J. Am. Chem. Soc.* **2009**, *131*, 18358.
- 11 Y. Duval, J. A. Mielczarski, O. S. Pokrovsky, E. Mielczarski, J. J. Ehrhardt, *J. Phys. Chem. B* **2002**, *106*, 2937.
- 12 L. T. Zhuravlev, *Colloids Surf., A* **2000**, *173*, 1.
- 13 J. P. Icenhower, P. M. Dove, *Geochim. Cosmochim. Acta* **2000**, *64*, 4193.
- 14 C. Park, P. A. Fenter, K. L. Nagy, N. C. Sturchio, *Phys. Rev. Lett.* **2006**, *97*, 016101.
- 15 A. M. Tikhonov, *J. Chem. Phys.* **2006**, *124*, 164704.
- 16 I. Danielewicz-Ferchmin, A. R. Ferchmin, *Phys. Chem. Chem. Phys.* **2004**, *6*, 1332.
- 17 D. A. Sverjensky, *Geochim. Cosmochim. Acta* **2005**, *69*, 225.
- 18 R. Varma, A. G. MacDiarmid, J. G. Miller, *Inorg. Chem.* **1964**, *3*, 1754.
- 19 F. H. J. van der Heyden, D. Stein, K. Besteman, S. G. Lemay, C. Dekker, *Phys. Rev. Lett.* **2006**, *96*, 224502.
- 20 G. R. Wiese, R. O. James, T. W. Healy, *Discuss. Faraday Soc.* **1971**, *52*, 302.